



## Climate change projections for the Mediterranean region

Filippo Giorgi <sup>a,\*</sup>, Piero Lionello <sup>b</sup>

<sup>a</sup> Earth System Physics Section, The Abdus Salam International Centre for Theoretical Physics, P.O. Box 586, (Strada Costiera 11 for courier mail), 34100 Trieste, Italy

<sup>b</sup> Università di Lecce, Lecce, Italy

### ARTICLE INFO

#### Article history:

Received 12 October 2006

Accepted 11 August 2007

Available online 4 October 2007

#### Keywords:

climate change

Mediterranean climate

precipitation change

temperature change

### ABSTRACT

We present a review of climate change projections over the Mediterranean region based on the most recent and comprehensive ensembles of global and regional climate change simulations completed as part of international collaborative projects. A robust and consistent picture of climate change over the Mediterranean emerges, consisting of a pronounced decrease in precipitation, especially in the warm season, except for the northern Mediterranean areas (e.g. the Alps) in winter. This drying is due to increased anticyclonic circulation that yields increasingly stable conditions and is associated with a northward shift of the Atlantic storm track. A pronounced warming is also projected, maximum in the summer season. Inter-annual variability is projected to mostly increase especially in summer, which, along with the mean warming, would lead to a greater occurrence of extremely high temperature events. The projections by the global and regional model simulations are generally consistent with each other at the broad scale. However, the precipitation change signal produced by the regional models shows substantial orographically-induced fine scale structure absent in the global models. Overall, these change signals are robust across forcing scenarios and future time periods, with the magnitude of the signal increasing with the intensity of the forcing. The intensity and robustness of the climate change signals produced by a range of global and regional climate models suggest that the Mediterranean might be an especially vulnerable region to global change.

© 2007 Published by Elsevier B.V.

### 1. Introduction

The Mediterranean region lies in a transition zone between the arid climate of North Africa and the temperate and rainy climate of central Europe and it is affected by interactions between mid-latitude and tropical processes. Because of these features, even relatively minor modifications of the general circulation, e.g. shifts in the location of mid-latitude storm tracks or sub-tropical high pressure cells, can lead to substantial changes in the Mediterranean climate. This makes the Mediterranean a potentially vulnerable region to climatic changes as induced, for example, by increasing concentrations of greenhouse gases (e.g. [Lionello et al., 2006a](#); [Ulbrich et al., 2006](#)). Indeed, the Mediterranean region has shown large climate shifts in the past ([Luterbacher et al., 2006](#)) and it has been identified as one of the most prominent “Hot-Spots” in future climate change projections ([Giorgi 2006](#)).

The climate of the Mediterranean is mild and wet during the winter and hot and dry during the summer. Winter climate is mostly dominated by the westward movement of storms originating over the Atlantic and impinging upon the western European coasts. The winter Mediterranean climate, and most importantly precipitation, is thus affected by the North Atlantic Oscillation (NAO) over its western areas

(e.g. [Hurrell 1995](#)), the East Atlantic (EA) and other patterns over its northern and eastern areas ([Trigo et al., 2006](#)). The El Niño Southern Oscillation (ENSO) has also been suggested to significantly affect winter rainfall variability over the Eastern Mediterranean (along with spring and fall precipitation over Iberia and North-western Africa, [Alpert et al., 2006](#)). In addition to Atlantic storms, Mediterranean storms can be produced internally to the region in correspondence of cyclogenetic areas such as the lee of the Alps, the Gulf of Lyon and the Gulf of Genoa ([Lionello et al., 2006b](#)).

In the summer, high pressure and descending motions dominate over the region, leading to dry conditions particularly over the southern Mediterranean. Summer Mediterranean climate variability has been found to be connected with both the Asian and African monsoons ([Alpert et al., 2006](#)) and with strong geopotential blocking anomalies over central Europe ([Xoplaki et al., 2004](#); [Trigo et al., 2006](#)).

In addition to planetary scale processes and teleconnections, the climate of the Mediterranean is affected by local processes induced by the complex physiography of the region and the presence of a large body of water (the Mediterranean Sea). For example, the Alpine chain is a strong factor in modifying traveling synoptic and mesoscale systems and the Mediterranean Sea is an important source of moisture and energy for storms ([Lionello et al., 2006a,b](#)). The complex topography, coastline and vegetation cover of the region are well known to modulate the regional climate signal at small spatial scales (e.g. [Lionello et al., 2006a](#)). In addition, anthropogenic and natural aerosols of central European, African and Asian origin can reach the

\* Corresponding author. Tel.: +39 040 2240 425; fax: +39 040 2240 449.

E-mail address: [giorgi@ictp.it](mailto:giorgi@ictp.it) (F. Giorgi).

## Subregions used in the analysis

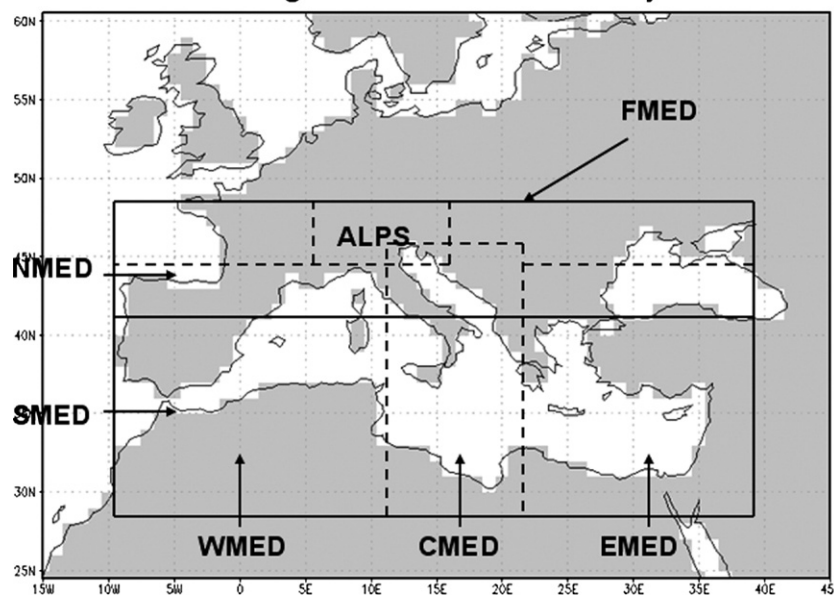


**Fig. 1.** Sub-regions used in the analysis presented in this paper. FMED = Full Mediterranean (28–48 N, 9.5 W–38.5 E); NMED = Northern Mediterranean (41–48 N, 9.5 W–38.5 E); SMED = Southern Mediterranean (28–41 N, 9.5 W–38.5 E); WMED = Western Mediterranean (28–44 N, 9.5 W–10.5 E); CMED = Central Mediterranean (28–46 N, 10.5–20.5 E); EMED = Eastern Mediterranean (28–4 N, 20.5–38.5 E); ALPS = Alpine region (44–48 N, 5.5–15.5 E). Grey shading indicates the land areas within the region in the common 1 degree CRU grid.

Mediterranean, possibly influencing its climate characteristics (Alpert et al., 2006). Because of the interactions of processes at a wide range of spatial and temporal scales, the climate of the Mediterranean is characterized by a great diversity of features, resulting in a variety of climate types and great spatial variability (Lionello et al., 2006a).

Despite the importance of this region within the global change context, assessments of climate change projections over the Mediterranean are relatively sparse. Perhaps the most comprehensive review of climate change projections over the Mediterranean region is reported by Ulbrich et al. (2006) based on a limited number of global and regional model simulations performed throughout the early 2000s. A number of papers have reported regional climate change simulations over Europe, including totally or partially the Mediterranean region (e.g. Giorgi et al., 1992; Rotach et al., 1997; Giorgi et al., 1997; Jones et al., 1997; Deque et al., 1998; Machenhauer et al., 1998; Raisanen et al., 1999; Christensen and Christensen 2003; Semmler and Jacob 2004; Schar et al., 2004; Giorgi et al., 2004b; Raisanen et al., 2004; Deque et al., 2005). Finally, several studies have presented regional evaluations of different generations of global model projections, including the Mediterranean region (Kittel et al., 1998; Giorgi and Francisco 2000; Giorgi et al., 2001, Giorgi and Bi 2005a,b). Reference will be made to these studies in the discussion of the results presented here.

The main motivation of this paper is that recent research efforts provide an opportunity to approach a Mediterranean climate change assessment on much stronger grounds than in the past. First, a worldwide effort has been recently carried out by which about 20 research groups around the world completed a large set of global climate simulations for the 20th and 21st century under different greenhouse gas forcing scenarios as a contribution to the fourth Assessment Report (AR4) of the Intergovernmental Panel on Climate Change (IPCC). Output from this ensemble of models, which is hereafter referred to as Multi Global Model Ensemble (or MGME), is stored at the Program for Climate Model Diagnosis and Intercomparison (PCMDI, <http://www-pcmdi.llnl.gov>) and is of public access. This dataset of unprecedented quality and comprehensiveness allows a much better assessment of climate change projections than in the past and has in fact spurred a large number of research projects on different climate change issues (see the PCMDI web site above).

The second effort we refer to is the completion of the European project Prediction of Regional scenarios and Uncertainties for Defining, European Climate change and associated risks and Effects (PRUDENCE, Christensen et al., 2002), in which a wide range of global and regional climate models were used to produce climate change projections over the European region. To complement this project, fine scale (grid interval of 20 km) multi-decadal regional simulations of climate change over the Mediterranean area have been completed by Gao et al. (2006).

Based on the availability of these new sources of information, which represent the state of the art in both global and regional climate change simulations, in this paper we present an updated assessment of future climate change projections over the Mediterranean basin. We examine different climate variables and statistics, such as mean changes and changes in variability and extremes for surface climate

**Table 1**

List of models, grid interval (atmosphere) and experiments used in this work. 20C indicates experiments for the 20th century, B1, A1B and A2, experiments for the 21st century under forcing deriving from the corresponding IPCC emission scenarios. The grid interval is approximate, as it may vary across latitudes and may be different in the longitude and latitude directions. The reader is referred to the PCMDI web site <http://www-pcmdi.llnl.gov> for more detailed information on models and experiments

Model	Grid interval	20	B1	A1	A2
CCMA-3-T47	~2.7°	5	4	4	2
CNRM-CM3	~2.8°	1	1	1	1
CSIRO-MK3	~2.3°	2	1	1	1
GFDL-CM2-0	~2.2°	3	1	1	1
GFDL-CM2-1	~2.2°	3	0	1	1
GISS-AOM	~3.5°	2	2	2	0
GISS-E-R	~4.5°	1	1	2	1
INMCM3	~4.5°	1	1	1	1
IPSL-CM4	~3.0°	1	1	1	1
MIROC3-	~1.2°	1	1	1	0
MIROC3-	~2.8°	3	3	3	3
MIUB-ECHO-G	~3.2°	5	3	3	3
MPI-	~2.3°	3	3	2	3
MRI-	~2.8°	5	5	5	5
NCAR-	~1.4°	8	8	6	4
NCAR-	~2.8°	4	2	3	4
UKMO-	~3.0°	1	1	1	1

variables as well as circulation patterns. We do not address issues of impacts, adaptation and mitigation, although we hope that our assessment might provide useful information for such issues.

Our assessment is based on both a new analysis of the above mentioned data and a review of published material deriving from the MGME and PRUDENCE data. Therefore, we begin this paper with a brief description of these datasets.

## 2. Definitions and datasets

In this paper we define the Mediterranean region as roughly encompassing the area between 28–48°N and 10°W–39°E (Fig. 1). It includes, fully or partially, over 20 countries (from the Alpine region in the north to the North African countries in the south, from the Iberian Peninsula in the west to the Middle East countries in the east) and a wide range of climatic types, from the north-African desert to the Alps.

Our assessment/analysis of global simulations with coupled Atmosphere–Ocean General Circulation Models (AOGCMs) utilizes what we have called the MGME. This is described in Table 1. It includes 17 models from laboratories around the World spanning a relatively wide range of resolutions, from 1 to 4°. Note that three of the original MGME models were neglected because they did not have simulations for the A1B scenario or because of their poor performance over the Mediterranean region (the FGOALS, BCC and HADGEM models).

The following simulations are available from the MGME dataset (see Table 1): 20 century climate using observed GHG and aerosol forcing (referred to as 20C experiments), 21st century climate using

GHG and aerosol forcing from the A1B, A2 and B1 emission scenarios of IPCC (1990) (referred to as A1B, A2 and B1 experiments, respectively). This set of scenarios spans almost the entire IPCC scenario range, with the B1 being close to the low end of the range (CO<sub>2</sub> concentration of about 550 ppm by 2100), the A2 to the high end of the range (CO<sub>2</sub> concentration of about 850 ppm by 2100) and the A1B to the middle of the range (CO<sub>2</sub> concentration of about 700 ppm by 2100). As shown in Table 1, some models include multiple realizations for the same experiment, in which case we utilize the ensemble average of the realizations.

Monthly data for the MGME experiments were obtained from the PCMDI web site (see above) and the reader is referred to this web site to obtain more information about the participating models. To facilitate the model inter-comparison, the data are interpolated onto a common 1-degree grid. A common 1-degree land mask grid is also defined (see Fig. 1), based on the half-degree grid of the observed dataset from the Climatic Research Unit (CRU) of the University of East Anglia (New et al., 2000). This implies that, when land-only or ocean-only analysis is presented, some uncertainty is present from the different land definitions at the different model grids. Except for two models, this is the same dataset used by Giorgi and Bi (2005a,b) and Giorgi (2006).

Because of the complex topography and coastlines of the Mediterranean basin, AOGCMs can only provide broad scale type of information. More detailed spatial information can be obtained from regional climate models, or RCMs, and therefore we examine results (mostly already published) from recent regional climate change simulations completed as part of the PRUDENCE project. This includes

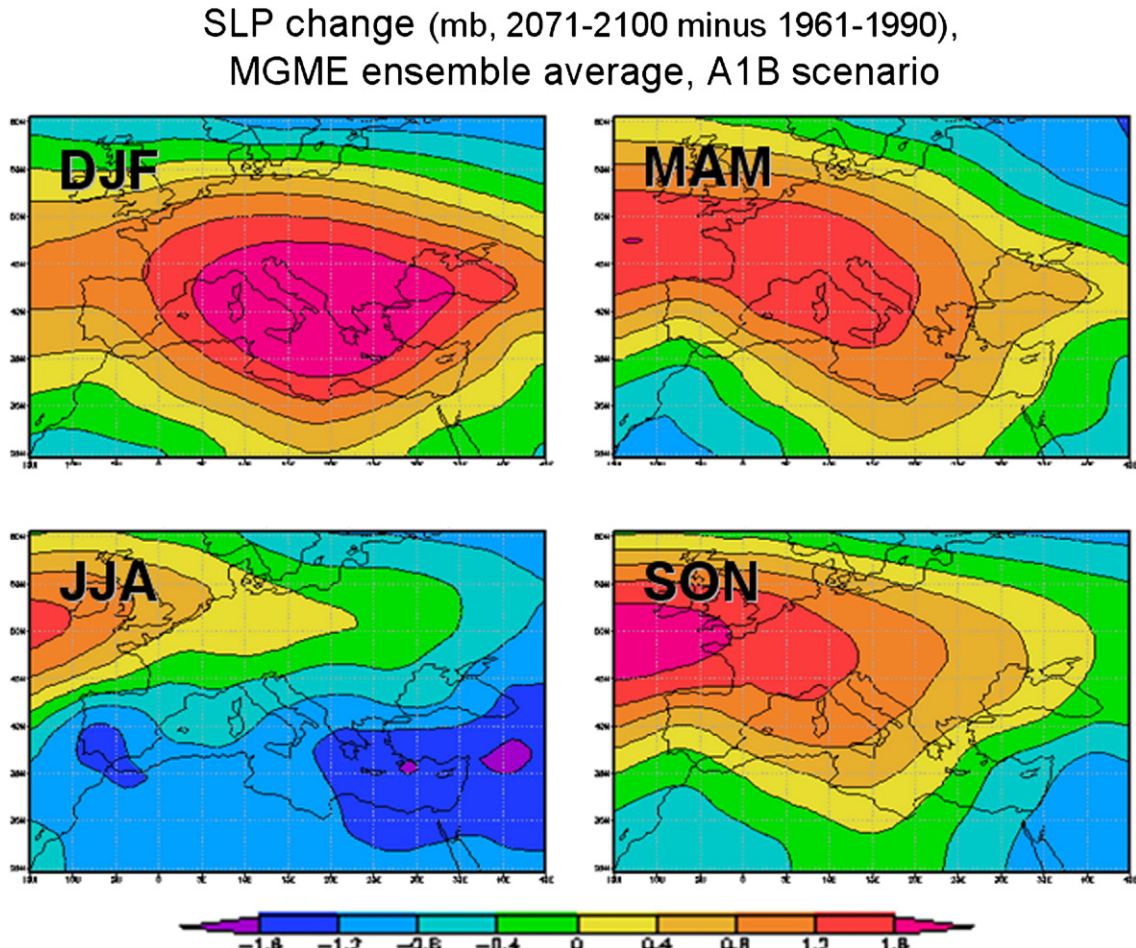


**Fig. 2.** MGME ensemble average change in sea level pressure (SLP) for the four seasons, 2071–2100 minus 1961–1990, A1B scenario. Units are mb. DJF is December–January–February, MAM is March–April–May, JJA is June–July–August, SON is September–October–November.

an ensemble of four AOGCMs and nine RCMs. The PRUDENCE RCM simulations are 30-year time slices, one for the present day reference period of 1961–1990, and the others for the future period of 2071–2100 with forcing from the A2 and B2 IPCC (2000) emission scenarios. Similar to the B1, the B2 scenario also lies towards the low end of the IPCC range, with a CO<sub>2</sub> concentration of about 620 ppm by 2100. The PRUDENCE RCM simulations cover the European region at a grid spacing of 50 km and are driven at the lateral boundaries by different global model forcing fields, although most of them utilize forcing from time-slice simulations completed with the Hadley Centre atmospheric model HadAM3H at a horizontal resolution of 1.25° × 2.75°. The reader is referred to the PRUDENCE web site (<http://www.dmi.dk/f+u/klima/prudence/>) for more information on the PRUDENCE project and experiment set up.

Finally, in order to address issues of fine scale structure of the climate change signal, we also review some results from recent simulations completed by Gao et al. (2006) in which a regional model (the RegCM of Giorgi et al., 1993a,b and Pal et al., 2000) was run at a grid spacing of 20 km for present day (1961–1990) and future (2071–2100, A2 and B2 emission scenarios) climate simulations for a region encompassing the Mediterranean basin. The regional model was used in the so-called double nested mode, i.e. it was driven at the lateral boundaries by meteorological fields obtained from the PRUDENCE simulations at 50 km grid spacing of Giorgi et al. (2004a,b).

### 3. Assessment of global model simulations

In this section we discuss climate change projections for the Mediterranean region as obtained from the MGME models. We

analyze mean change patterns over the Mediterranean (Section 3.1), changes over different Mediterranean sub-regions (Section 3.2) and changes in inter-annual variability (Section 3.3).

#### 3.1. Mean changes

Figs. 2–5 first show the ensemble average change in seasonal sea level pressure (SLP), 500 hPa geopotential height (Gph), precipitation and surface air temperature for the period 2071–2100 and the A1B scenario compared to 1961–1990 over the European region. Note that the changes in 500 hPa Gph are always positive because the atmosphere below 500 hPa is warmer, and thus thicker, in the future scenarios than present day conditions. What matters in terms of the circulation are the horizontal gradients in the changes of 500 hPa Gph.

In DJF the models show an area of increased SLP (Fig. 2), and thus increased anticyclonic circulation, centered over the central Mediterranean, with a pronounced ridge in the 500 hPa Gph change pattern. In the other seasons, the area of increased SLP and 500 hPa Gph extends from the northeastern Atlantic to central Europe and the Mediterranean. The main effect of this circulation change pattern is a northward shift of the Atlantic storm track, with a deflection of storms north of the Mediterranean region into higher latitude areas. We also note that increased high pressure and anticyclonic conditions generally lead to greater stability and thus conditions less favorable to storm generation.

As a consequence of these circulation change patterns the Mediterranean region exhibits a general reduction in precipitation, while the northern European regions show an increase in

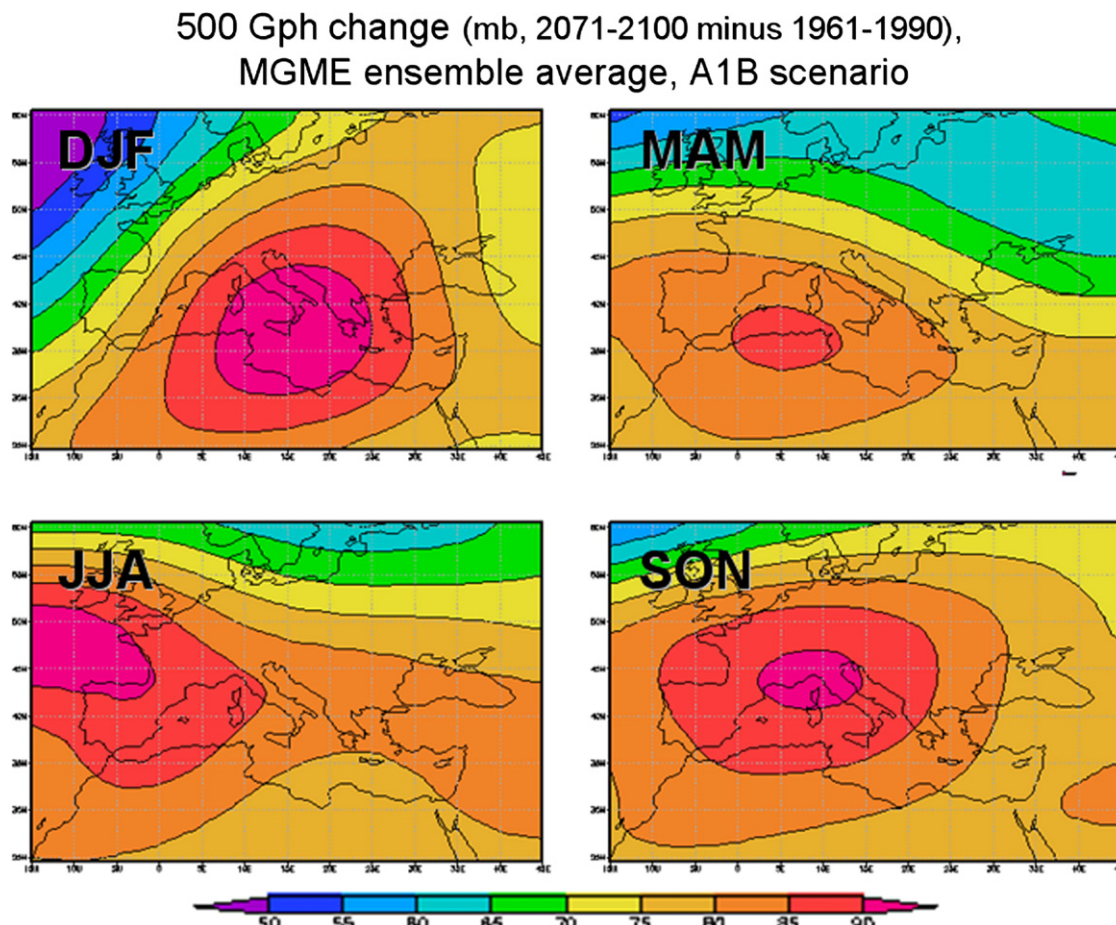


**Fig. 3.** MGME ensemble average change in 500 hPa geopotential height (Gph) for the four seasons, 2071–2100 minus 1961–1990, A1B scenario. Units are m. DJF is December–January–February, MAM is March–April–May, JJA is June–July–August, SON is September–October–November.

## Precipitation change (%, 2071–2100 minus 1961–1990), MGME ensemble average, A1B scenario

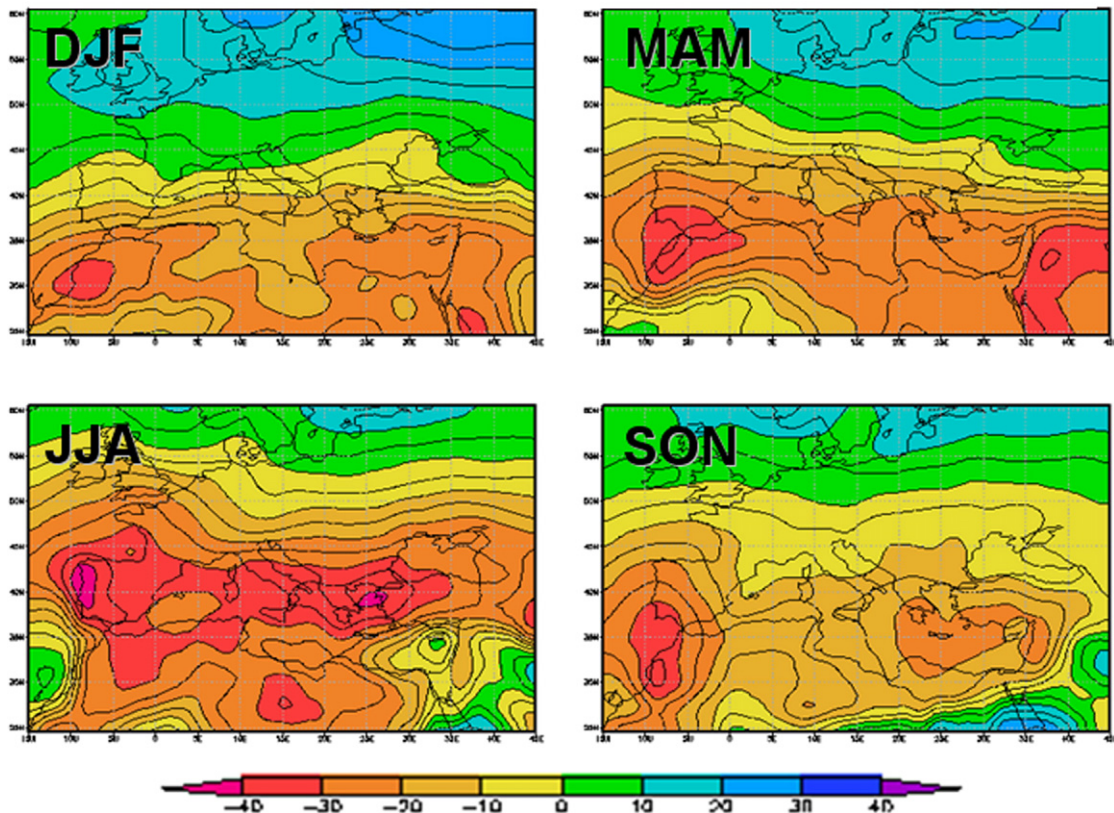


**Fig. 4.** MGME ensemble average change in precipitation for the four seasons, 2071–2100 minus 1961–1990, A1B scenario. Units are % of 1961–1990 value. DJF is December–January–February, MAM is March–April–May, JJA is June–July–August, SON is September–October–November.

precipitation (Fig. 4). The area of precipitation reduction has a maximum northward extension in the summer, encompassing most of the western European continental areas, consistently with the SLP and 500 Gph change patterns, which present their largest positive values over the northeast Atlantic in this season. In JJA, MAM and SON essentially the entire Mediterranean region and most of Western Europe show a pronounced decrease in precipitation. In winter the transition area between positive and negative precipitation change moves southward and crosses the northern Iberian, Italian and Balkan peninsulas. In the east–west direction we find that the largest precipitation reduction occurs over the western and eastern Mediterranean, partially in association with local topographical features (such as the Iberian Plateau and Atlas mountains in the west and the Balkan peninsula in the East), with a more irregular inter-seasonal behavior in the east.

Concerning temperature (Fig. 5), the Mediterranean region exhibits a warming maximum in summer. In winter and spring, the maximum warming magnitudes are found over continental northeastern Europe, at least partially in response to reduced snow cover there. In the fall the warming is more equally distributed throughout the European land areas. In general the mitigating effect of the Mediterranean Sea and the reduced warming over the sea areas is present in all seasons.

Figs. 2–5 thus give us an overall picture of increasingly drier and warmer conditions over the Mediterranean in the future climate scenarios, with this pattern being particularly pronounced in the summer season. These results are generally consistent with previous studies using both this ensemble of models (Giorgi and Bi, 2005b) and previous generations of AOGCM simulations (Kittel

et al., 1998; Giorgi and Francisco 2000; Giorgi et al., 2001; Ulbrich et al., 2006).

The patterns of SLP, precipitation and temperature change shown in Figs. 2–5 are robust across scenarios and future periods. For example, Figs. 6 and 7 show the ensemble average precipitation change patterns for the B1 and A2 scenarios and the same time period (2071–2100) while Fig. 8 shows the DJF and JJA changes for the A1B scenario but different time slices (2011–2040 and 2041–2070). The patterns are remarkably similar in shape but with different magnitudes tied to the greenhouse gas forcing: the higher the forcing the larger the magnitude of change. It is worth noting that this result, which has been found in previous studies (e.g. Mitchell 2003; Giorgi, 2005) is not obvious, especially for precipitation, since both the GHG and aerosol forcings vary markedly across time slices and scenarios.

### 3.2. Sub-regional analysis

For a more quantitative analysis of the MGME simulations we divide the Mediterranean area into a number of sub-regions (see Fig. 1) and investigate results for the sub-regional averages. Before showing the change projections over these sub-regions we analyze the performance of the MGME over our area of interest. To do so we compare the MGME climatology over the various Mediterranean sub-regions to the CRU observations by including only land grid points based on the CRU land mask. Also, in order to assess issues of multi-decadal variability and temporal trends, in our sub-regional analysis we examine averages for 20-year periods (rather than 30 years). As a reference period we use 1961–1980 since this is the latest period of

## Temperature change (C, 2071-2100 minus 1961-1990), MGME ensemble average, A1B scenario

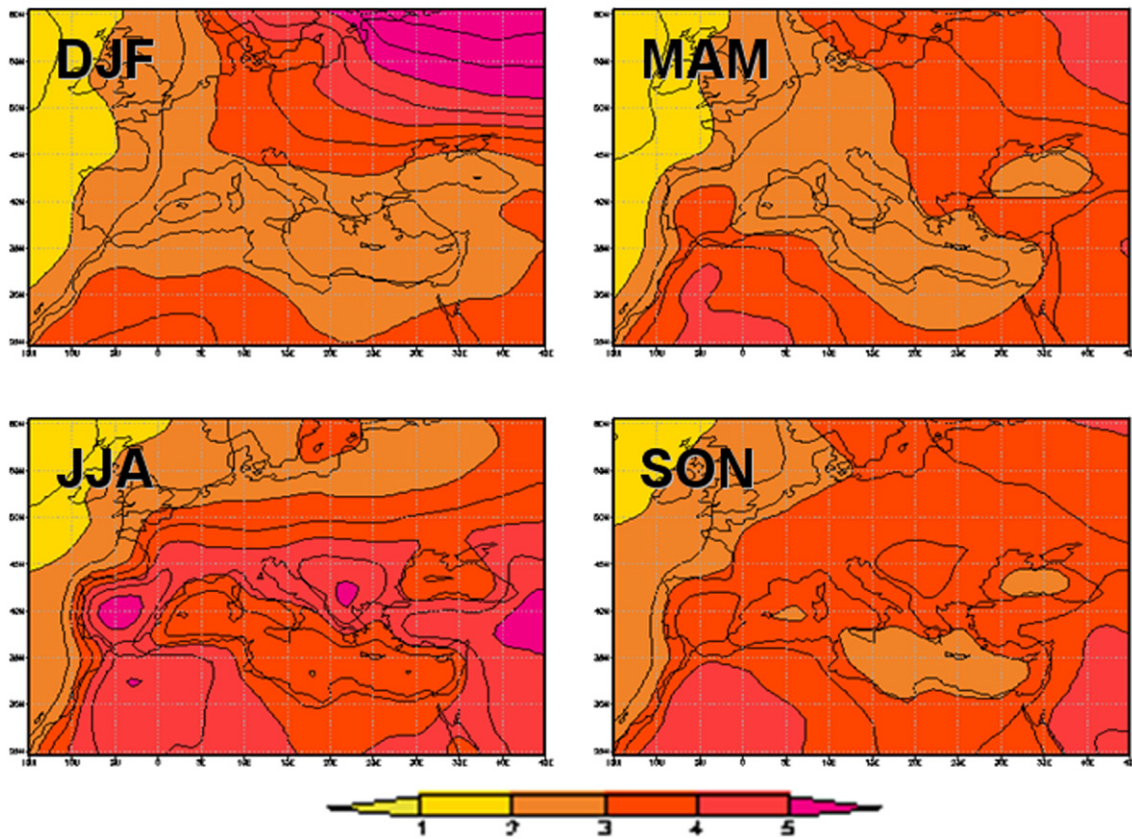


**Fig. 5.** MGME ensemble average change in surface air temperature for the four seasons, 2071–2100 minus 1961–1990, A1B scenario. Units are °C. DJF is December–January–February, MAM is March–April–May, JJA is June–July–August, SON is September–October–November.

the 20th century in which the anthropogenic signal is not dominant (e.g. Mitchell et al., 2001).

Fig. 9 shows the seasonal precipitation and temperature biases for the full MGME over the full Mediterranean region and the 6 sub-regions of Fig. 1 for the reference period 1961–1980. Although we only present biases for the 1961–1980 period, the biases for other 20-year periods of the 20th century have similar values. It is evident that, as an ensemble, the MGME reproduces well the observed climatology of the region. Precipitation is mostly underestimated, but in the majority of cases the biases are less than 20% in magnitude. In addition, the biases do not vary much for the different sub-regions and seasons, which indicates that both the contrast between semi-arid southern areas and northern wet alpine areas and the seasonal cycle of precipitation, with a winter maximum and a summer minimum, are captured by the simulations. This gives good confidence on the capability of the models to simulate correctly the climate change signal. The only instances of relatively high precipitation bias, over 40%, occur in the summer over the southern and western Mediterranean. However, summer precipitation over these regions is extremely small and this inflates the percentage bias.

The temperature biases for the MGME are also generally small, mostly less than 1 °C. The ensemble of models appears to predominantly underestimate temperature, with cold biases especially in the intermediate seasons (MAM and SON). The largest positive ensemble biases, in excess of 1 °C, occur over the Alps and northern Mediterranean region and might be tied to an underprediction of winter snow cover at the relatively coarse model resolutions.

As also indicated in IPCC (2001), the last decades of the 20th century showed trends in some climate variables, most noticeably temperature, likely attributable to anthropogenic greenhouse gas forcing. As an attempt to assess whether the MGME at least qualitatively captures these trends over the Mediterranean region, Fig. 10 compares the differences in Mediterranean seasonal precipitation and temperature between the last 2 decades of the century (1981–2000) and the reference period 1961–1980 in the CRU dataset and in the MGME.

The CRU observed precipitation over the Mediterranean shows a decrease in 1981–2000 in DJF, MAM and JJA, while it shows a small increase in SON. The DJF decrease has been attributed to the influence of an increasingly positive phase of the NAO which occurred in the late decades of the 20th century (Hurrell 1995). The MGME does not reproduce the changes found in the CRU observations except for the summer drying. The ability of model projections to simulate this summer drying trend consistently with CRU observations was also found by Pal et al. (2004).

The disagreement between observed and simulated precipitation trends in winter and spring deserves some specific discussion. On the one hand, this is not necessarily an indication of poor model performance. It could simply be an indication that the observed precipitation changes are not related to greenhouse gas forcing but are due to natural variability. The largest contribution to the total Mediterranean precipitation comes from the northern areas, where precipitation presents a negative correlation with the NAO phase. The increase in the positive NAO phase and the associated decrease of precipitation in the 1980s and 90s could simply be a random

## Precipitation change (%), 2071–2100 minus 1961–1990, MGME ensemble average, B1 scenario

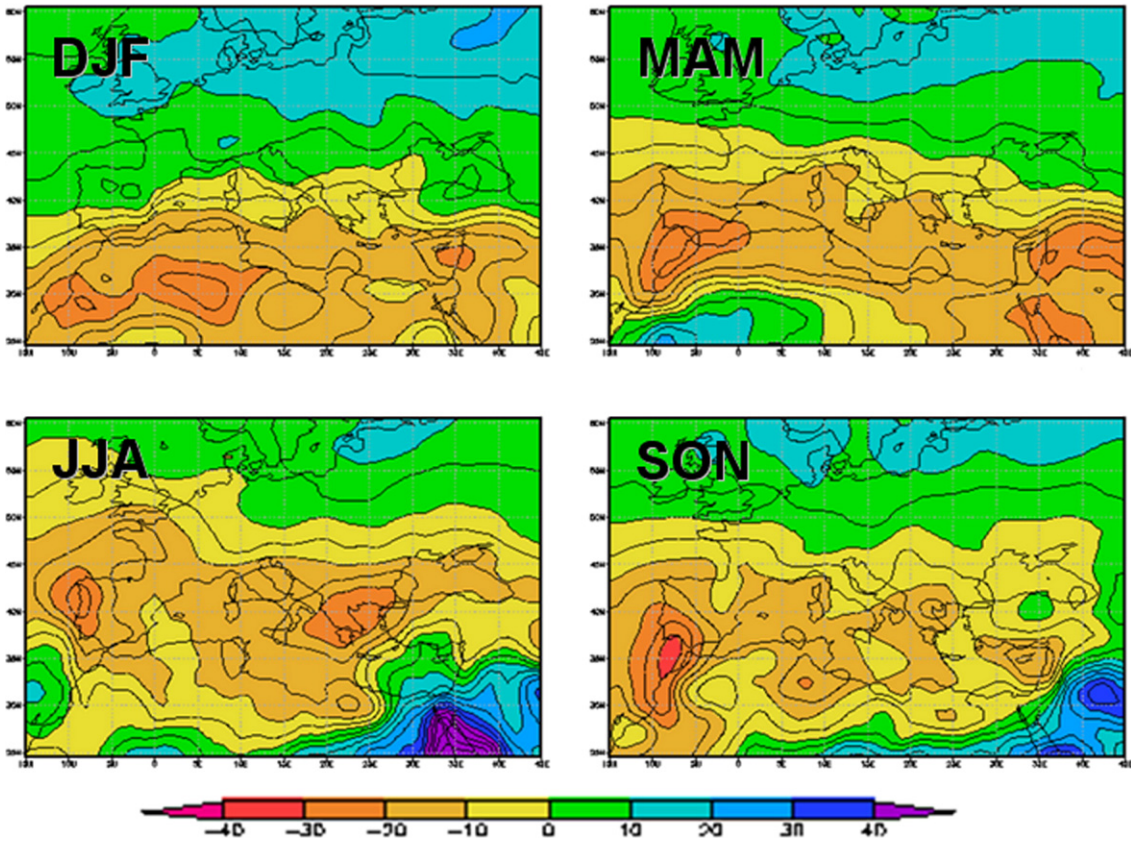


**Fig. 6.** MGME ensemble average change in precipitation for the four seasons, 2071–2100 minus 1961–1990, B1 scenario. Units are % of 1961–1990 value. DJF is December–January–February, MAM is March–April–May, JJA is June–July–August, SON is September–October–November.

multi-decadal event. On the other hand a shift of NAO towards positive values is suggested by several scenario simulations (e.g. Terray et al., 2004; Coppola et al., 2005), and the disagreement between observed and simulated precipitation trends could show an inadequate reproduction by the models of the early stage of this behavior. It should also be added that some uncertainty is present in precipitation observations, especially in areas of sparse station density, so that the changes indicated by the CRU dataset should be taken with caution. However, while the trends in the other seasons are generally found not to be significant in other datasets, the winter reduction of precipitation is generally confirmed (Jacobbeit et al., 2005; Xoplaki 2002; Xoplaki et al., 2004). We finally note that the models and observations show opposite precipitation trends in Autumn (Fig. 10), although these trends are relatively small.

Surface warming in the late 20th century has been clearly associated to greenhouse gas forcing, both at the global (Mitchell et al., 2001) and sub-continental (Stott, 2003) scales. Fig. 10 indeed shows that the MGME captures the observed late 20th century warming and in particular its seasonality (maximum in summer and minimum in winter). This gives encouraging indications towards the use of the MGME for climate change projections over the region.

Moving now our attention to the projections for the 21st century, Fig. 11 first shows the projected changes (A1B scenario compared to 1961–1980) in surface air temperature and precipitation by the model ensemble over the entire Mediterranean region for different 20-year periods. Consistently with Figs. 4 and 5, for both variables the change

signal persists of the same sign and increases in magnitude throughout the century in response to increased greenhouse gas forcing. For the whole basin, precipitation decreases in all seasons and periods. Summer shows the greatest decrease, from about -7% in 2001–2020 to ~-28% in 2081–2100. In the other seasons the decreases are ~-2 to -8% in DJF, -2 to -14% in MAM and -3 to -15% in SON. The surface warming also steadily increases throughout the century, being maximum in summer (~1.2 in 2001–2020 to 4.6 in 2081–2100) and minimum in winter (~0.7 to 3.1 °C). Fig. 11 thus clearly shows that summer is the most responsive season to greenhouse gas forcing over the Mediterranean.

Also shown in Fig. 11 is the inter-model variability of the change signal as measured by the standard deviation of the changes simulated by each individual model. With one exception (precipitation in DJF), the inter-model standard deviation (and therefore the inter-model spread) increases with time and thus with forcing and intensity of the signal. In other words, the models tend to deviate more from each other as the simulation progresses and the forcing and change signals increase. The seasonality of the standard deviation also generally follows the seasonality of the signal, with a marked summer maximum.

In terms of magnitude, the temperature inter-model standard deviation is much smaller than the ensemble average warming signals, indicating that the signals are robust. For precipitation, the inter-model standard deviation of the seasonal precipitation is generally smaller than the signal in the late decades of the 21st century. In particular, the summer drying signal for the decades 2081–2100 is more than twice as large as the corresponding inter-model

## Precipitation change (%, 2071–2100 minus 1961–1990), MGME ensemble average, A2 scenario

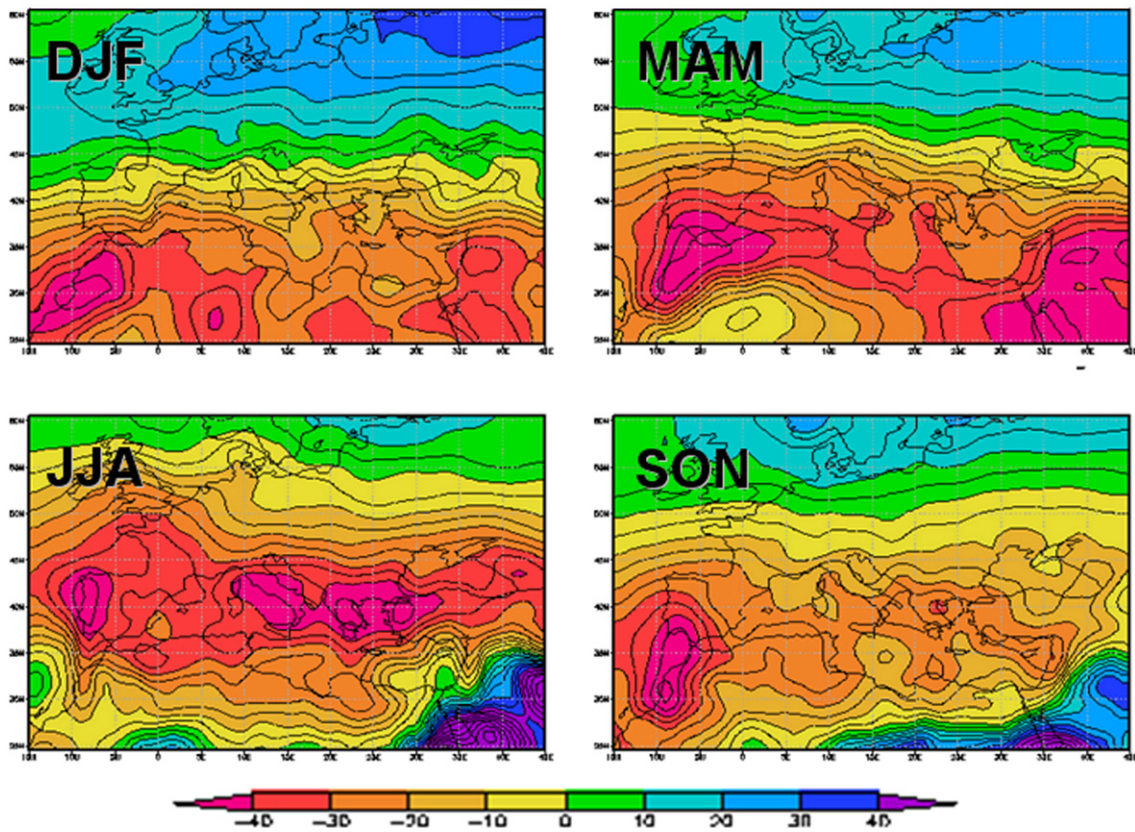


**Fig. 7.** MGME ensemble average change in precipitation for the four seasons, 2071–2100 minus 1961–1990, A2 scenario. Units are % of 1961–1990 value. DJF is December–January–February, MAM is March–April–May, JJA is June–July–August, SON is September–October–November.

standard deviation, showing that almost all models agree in projecting drying over the region.

The sensitivity of the changes to the forcing scenarios is shown in Fig. 12. Again we see the same signal in all scenarios (precipitation decrease and surface warming) with magnitude increasing with increasing greenhouse gas forcing: the A2 scenario shows the largest changes while the B1 shows the smallest. The seasonality of the changes (maximum in summer and minimum in winter) is retained in all scenarios. Note that the changes are large particularly in the summer, over 4 °C warming and over –25% precipitation reduction, for the A1B and A2 scenarios.

Fig. 13 shows a comparison of precipitation and temperature changes for land and sea areas in the Mediterranean domain. The sign and seasonality of the changes are the same over land and sea. As already noted, the warming is larger over land than over sea (by about 1° in all seasons). Conversely, the precipitation decrease is more pronounced over the sea areas, despite the greater evaporation from the sea in the future warmer climate conditions. The pronounced decrease over sea could be due to the greater distance of most of the Mediterranean Sea surface from the northward shifted storm track and from the areas where the topographic effect on cyclogenesis and precipitation remains large in the future climate scenarios.

The disaggregation of the precipitation and temperature change signals by sub-regions within the Mediterranean (see Fig. 1) for the A1B scenario is given in Fig. 14. The temperature change signal is essentially the same in the northern and southern Mediterranean in all seasons (Fig. 14), with maximum differences of only a few tenths of a degree. For precipitation however, the northern and southern Mediterranean change signals show some important differences. In

MAM, JJA and SON both sub-regions exhibit a precipitation decrease, but this is much more pronounced over the southern Mediterranean region. In DJF, this different behavior is more marked, with the southern Mediterranean showing a substantial drying (about –20% for the A1B scenario), while the northern Mediterranean shows essentially no change. These differences in the behavior of the southern and northern Mediterranean areas can be ascribed to the seasonal oscillation of the region of increased anticyclonic circulation discussed above (see Fig. 2) and to the mitigating role of the Alps.

Fig. 14 analyzes the Mediterranean along sub-regions in the east–west direction, with the Alps being treated separately. Again the temperature change signal shows only modest variability across regions (less than a half degree), with the warming being slightly more pronounced over the western Mediterranean (except for winter). Greater differences are found for precipitation. Consistently with what found in the case of the northern Mediterranean sub-region, the Alps show the least pronounced drying in MAM, JJA and SON and an increase of precipitation in DJF. The other regions show a drying signal in all seasons, least pronounced over the central Mediterranean. This different behavior of the central Mediterranean area is consistent with the role of the Alps in mitigating the change towards drier climate, which does not reach the eastern and western Mediterranean areas.

### 3.3. Changes in inter-annual variability

Previous analyses of the MGME have also addressed the issue of changes in inter-annual variability (Giorgi and Bi 2005a; Giorgi 2006). This was measured by the inter-annual standard deviation for

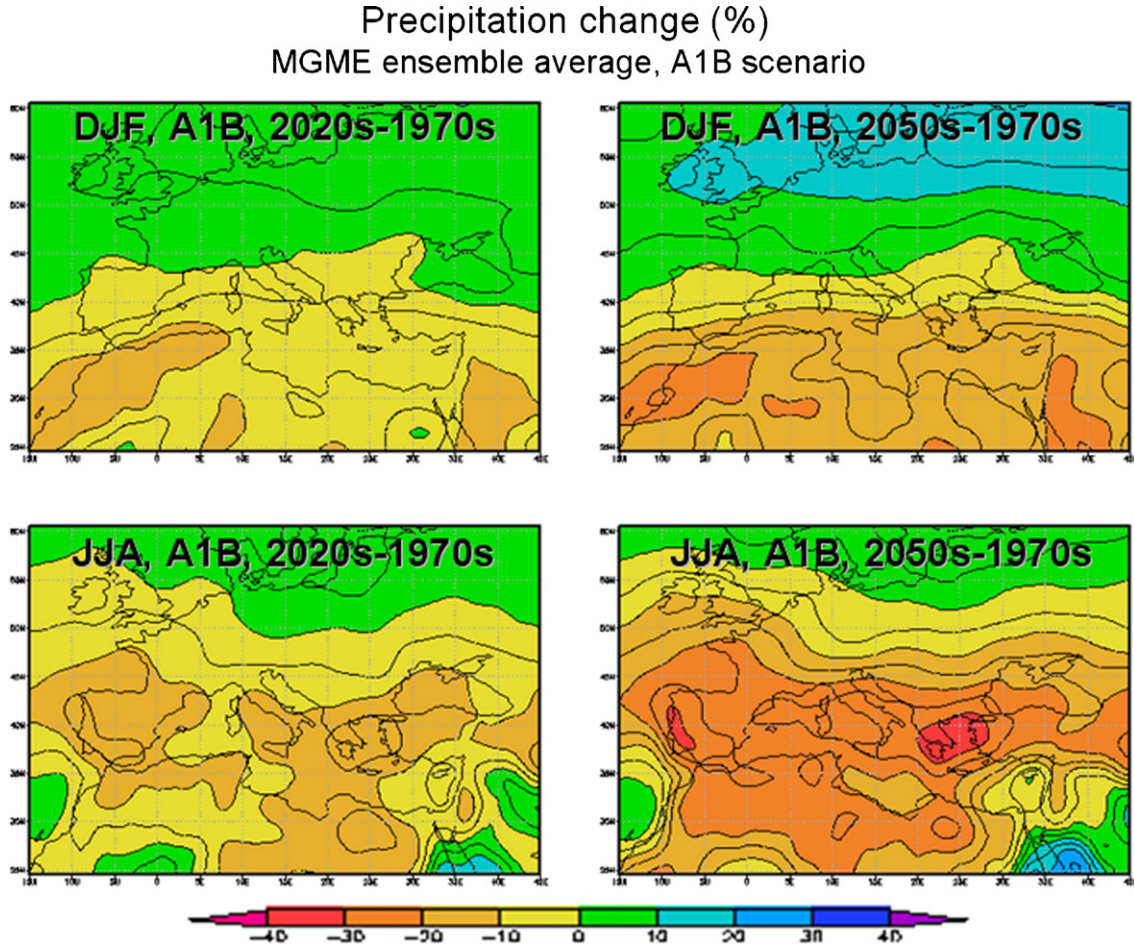


**Fig. 8.** MGME ensemble average change in precipitation for the four seasons and different future time periods. Units are % of 1961–1990 value. 1970s is 1961–1990, 2020s is 2011–204, 2050s is 2041–2070, 2080s is 2071–2100.

temperature and the coefficient of variation (standard deviation divided by the mean) for precipitation. In the latter case, use of the coefficient of variation removes the well known dependency of the precipitation standard deviation on the mean. The results for the entire Mediterranean region are summarized in Table 2 for 6-month periods covering the wet/cold season (October–March, or O–M) and dry/warm season (April–September, or A–S).

For precipitation we find a general increase in variability during both the wet/cold season and the dry/warm season, therefore this increase is found regardless of the magnitude of changes in mean precipitation. Similarly to the mean, the magnitude of the change in precipitation variability generally increases with the intensity of the forcing, i.e. they increase with time in the 21st century and are minimum in the B1 scenario. Table 2 also shows that the precipitation variability change signal is greater in the dry season than the wet season and that it becomes substantial only in the late decades of the century. This increase in precipitation variability appears to be generally consistent with an intensified hydrological cycle expected under warmer conditions. During wet periods the precipitation intensities increase in response to greater atmospheric water holding capacity while the wet periods are separated by longer dry periods due to feedback with generally drier land areas (IPCC 2001).

For temperature, we find a different variability change signal in the warm and cold seasons. In the warm season the inter-annual variability increases, which is consistent with the increase in precipitation variability and the associated feedbacks between the surface water and energy budgets. The increase in variability, along with the large mean warming, is expected to produce a much more

frequent occurrence of extremely high temperature events and heat waves (Schar et al., 2004). In the cold season the temperature variability shows only small changes, and mostly negative in the late decades of the century. This has been at least partially attributed to the decrease of snow cover under warmer conditions, which decreases the effectiveness of the snow-albedo feedback mechanism (Raisanen 2002; Giorgi and Bi 2005a).

#### 4. Assessment of the PRUDENCE simulations

In this section we review results of regional climate projections for the European region, including the Mediterranean, produced within the framework of the PRUDENCE project. The PRUDENCE strategy entails the use of multiple scenarios (A2 and B2), multiple GCMs (4) and multiple RCMs (9) to assess issues of uncertainty in regional climate change projections over Europe. Different RCMs were driven at the lateral boundaries by either the same or different GCMs. Most PRUDENCE simulations covered the future climate period 2071–2100 under the A2 and B2 IPCC scenarios and the changes were calculated with respect to the present day period 1961–1990. It should be noted that, unfortunately, most PRUDENCE RCM domains did not include the extreme eastern and southern areas of the Mediterranean.

##### 4.1. Mean changes

Fig. 15 summarizes the projections by the PRUDENCE full ensemble of models (both regional and global) over different sub-regions of Europe (adapted from Deque et al., 2005), and in particular it reports

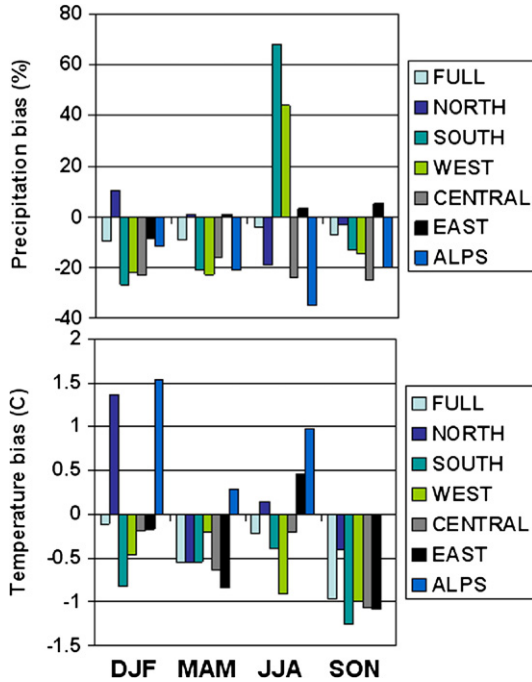


**Fig. 9.** MGME ensemble average precipitation (% of present day value, upper panel) and surface air temperature (°C) bias for the period 1961–1980 and the sub-regions of Fig. 1. The bias is calculated with respect to CRU land observations.

the range of projections by the PRUDENCE ensemble including all models and scenarios. These projections can be roughly compared with those obtained from the MGME, although the comparison is somewhat limited by the fact that the definition of the PRUDENCE regions is not the same as the one we adopted in Section 3. A broad agreement between the PRUDENCE and MGME projections over the Mediterranean region can be observed. The summer drying and maximum warming in all Mediterranean sub-regions is evident also in the PRUDENCE projections. The only discrepancy with the MGME data seemingly occurs when comparing the winter precipitation change over the Iberian Peninsula in PRUDENCE (Fig. 15) with that produced by the MGME over the western European region (Fig. 14). While the former shows a (small) increase, the latter shows a decrease, i.e. the area of increased precipitation extends farther south in the PRUDENCE models than in the MGME. An important aspect of the results in Fig. 15 is that in nearly every case all models agree on the sign of the precipitation change signal.

Fig. 16 addresses the issue of the relative importance of the source of uncertainty in the simulated range of change projections. This figure is derived from the data reported by Deque et al. (2005), who disaggregated the projection uncertainty (as defined by the range of model projections) into four sources: different GCMs, RCMs and scenarios, and internal GCM variability (i.e. variability associated with different realizations of the same scenario simulation). In evaluating the results in Fig. 16, it should be kept in mind that the PRUDENCE scenarios only cover about half of the full IPCC range and the PRUDENCE GCMs are only a small set of the full MGME set.

Fig. 16 first shows that, both for temperature and precipitation, the internal model variability is a minor source of uncertainty in all seasonal cases and both for temperature and precipitation. In general, for temperature the uncertainty due to the use of different GCMs represents the largest contribution to the total uncertainty range, followed by that associated with the scenarios. The uncertainty associated with the use of different RCMs (for the same boundary forcing) is secondary for temperature, implying that the boundary forcing is dominant in determining the temperature RCM response, at least at the European-wide scale.

Different conclusions are however found for precipitation. Especially in summer, when local processes (e.g. convection) and sub-regional circulation features are more important than in winter, the contribution to the total uncertainty deriving from the use of different RCMs is comparable to that associated with GCM boundary conditions and scenarios. This implies that the internal RCM physics and dynamics are as important as the boundary forcing in determining precipitation. A consequence of this result is that ensembles of RCM simulations (for the same GCM boundary forcing) may be needed to assess the uncertainty in simulated climate change projections over Europe.

#### 4.2. Changes in variability, extremes and storms

A primary advantage of using RCMs is that their increased resolution should allow a better simulation of variability and extremes. A few of studies within the PRUDENCE project addressed the issue of projected changes in variability and extremes over Europe. Inter-annual variability in the control and future climate simulations was analyzed for example by Giorgi et al. (2004b) and Schar et al. (2004). They found that, especially during the summer, inter-annual variability increased over the Mediterranean region in the scenario runs, a result in general agreement with what found in the MGME. In particular, Schar et al. (2004) pointed out how the increase of summer variability in conjunction with the mean warming would lead to much more frequent heat waves of magnitude similar or even greater than that occurred in the summer of 2003.

Changes in extreme events were analyzed by Christensen and Christensen (2003), Pal et al. (2004), Semmler and Jacob (2004), Kjellstrom (2004), Sanchez et al. (2004), Beniston et al. (2007) and Kjellstrom et al. (2007). High temperature extremes and drought events were found to increase substantially in summer while winter low temperature extremes were found to decrease (Beniston et al., 2007; Kjellstrom 2004; Kjellstrom et al., 2007). Concerning

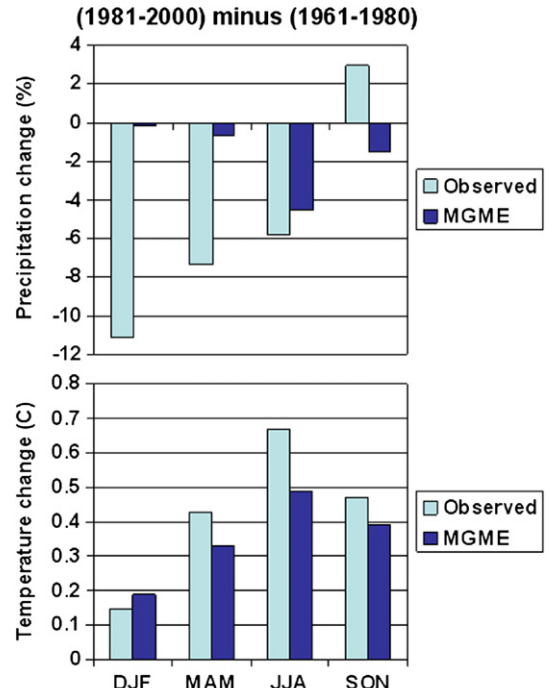


**Fig. 10.** Observed (CRU data) and MGME ensemble average change in precipitation (upper panel) and surface air temperature (lower panel) for the four seasons over the full Mediterranean region (see Fig. 1), land only, 1981–2000 minus 1961–1980. Units are % of 1961–1980 value for precipitation and °C for temperature.

### MGME ensemble average, A1B scenario

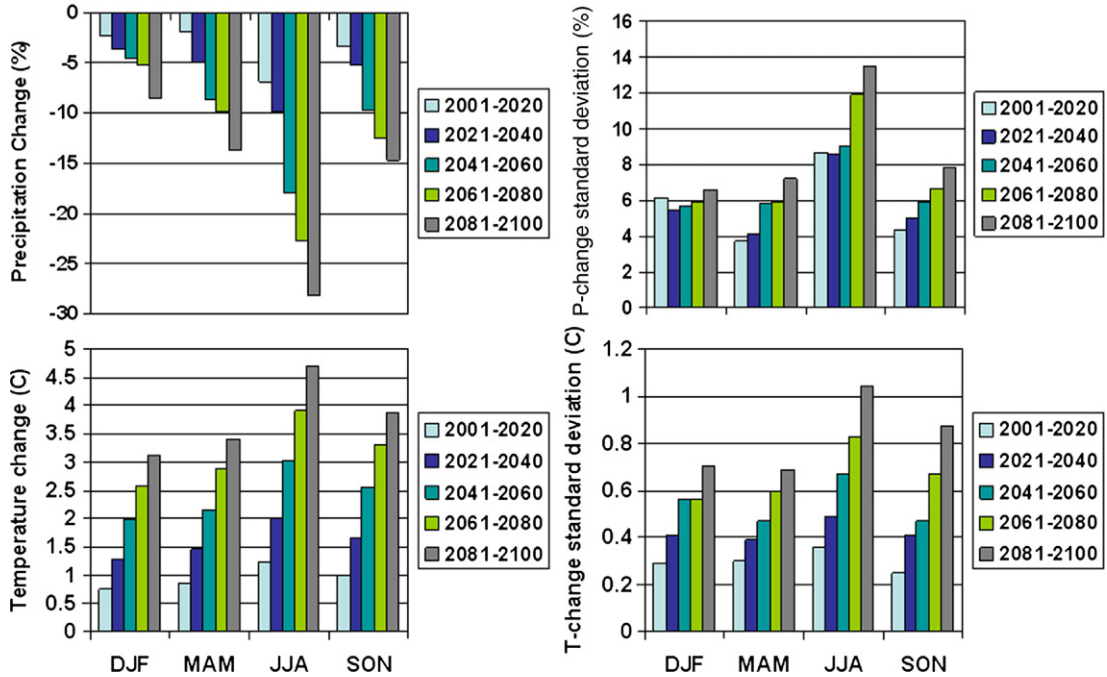


**Fig. 11.** MGME ensemble average change in mean precipitation (upper left panel), precipitation inter-model standard deviation (upper right panel), mean surface air temperature (lower left panel) and surface air temperature inter-model standard deviation (lower right panel) for the full Mediterranean region (see Fig. 1), the four seasons and different future time periods. The changes are calculated with respect to the 1961–1980 reference period and include only land points. Units are % of 1961–1980 value for mean precipitation, coefficient of variation and standard deviation, and °C for mean temperature.

precipitation, the overall substantial decrease in the summer mean was not accompanied by a corresponding decrease in the intensity of events, but rather a decrease in their frequency. In particular, the

frequency of extreme summer precipitation events increased over large regions of the Mediterranean (Christensen and Christensen 2003; Pal et al., 2004). These results imply not just a an overall

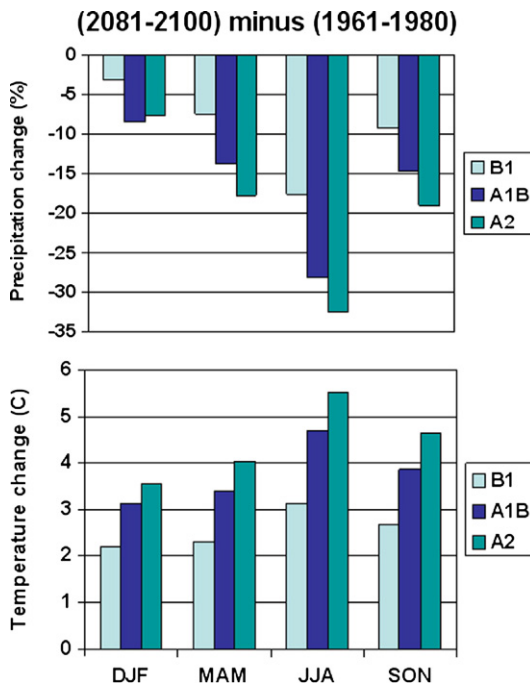


**Fig. 12.** MGME ensemble average change in mean precipitation (upper panel) and mean surface air temperature (lower panel) for the full Mediterranean region (see Fig. 1), the four seasons and different scenario. The changes are calculated between the periods 2081–2100 and 1961–1980 and include only land points. Units are % of 1961–1980 value for precipitation and °C for temperature.

### (2081-2100) minus (1961-1980), A1B scenario

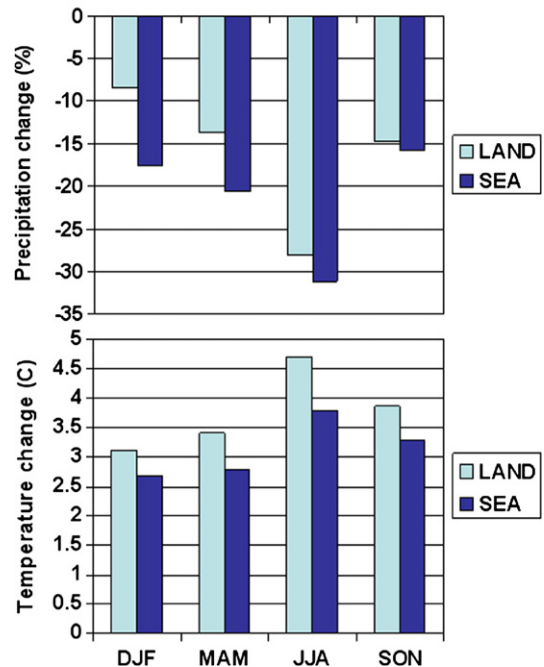


**Fig. 13.** MGME ensemble average change areas in mean precipitation (upper panel) and mean surface air temperature (lower panel) over land and sea areas within the full Mediterranean region (see Fig. 1) and the four seasons. The changes are calculated between the periods 2081–2100 and 1961–1980. Units are % of 1961–1980 value for precipitation and °C for temperature.

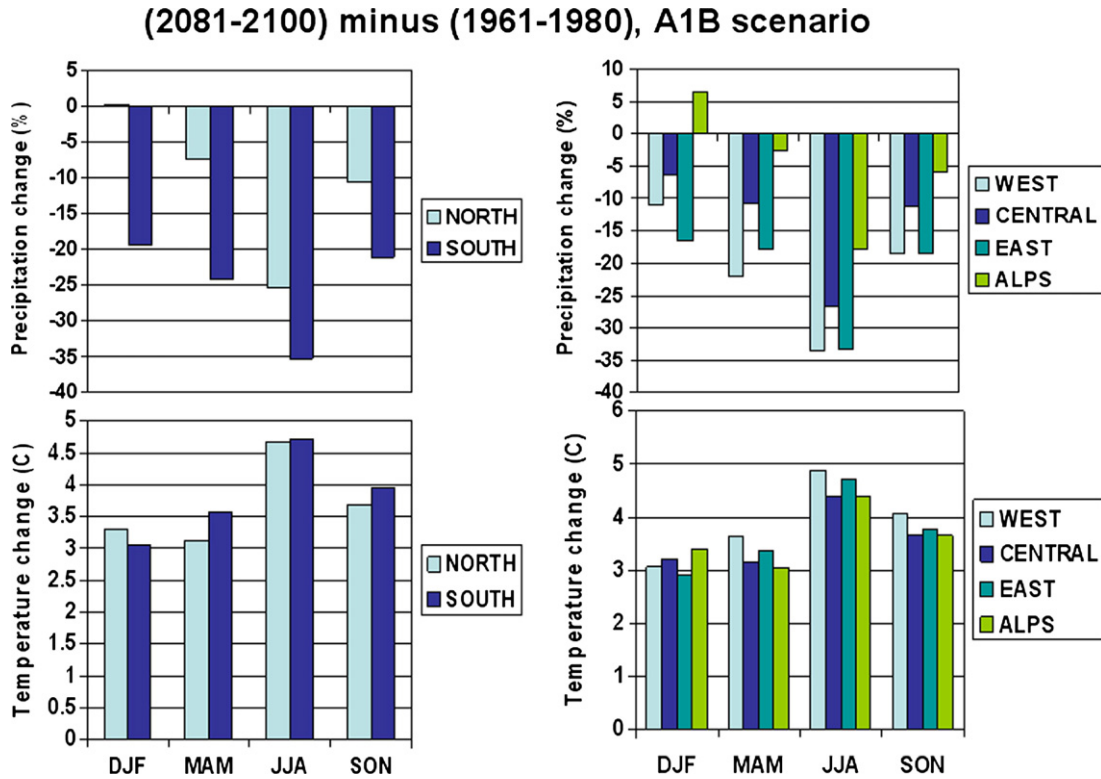


**Fig. 14.** MGME ensemble average change in mean precipitation (upper panels) and mean surface air temperature (lower panels) for the different Mediterranean sub-regions of Fig. 1, the four seasons and the A1B scenario. The changes are calculated between the periods 2081–2100 and 1961–1980 and include only land points. Units are % of 1961–1980 value for precipitation and °C for temperature.

decreased probability of precipitation but also a change of shape of its probability distribution, with an increased skewness determining at the same time higher probability for intense events and a lower value of average precipitation. On a yearly basis, a prevailing increase in precipitation extremes over the Mediterranean was found, particularly over and around the Alpine region, by Beniston et al. (2007) and Semmler and Jacob (2004).

The RCM simulations by Giorgi et al. (2004a,b) were used for an analysis of changes in different cyclone statistics under A2 scenario conditions by Lionello et al. (2006a,b). Among these statistics were the synoptic signal (the standard deviation of the 1–7 day band pass filtered sea level pressure maps) and the cyclone trajectories. For the Mediterranean region the results suggested a weaker synoptic signal than in present climate (Lionello et al., 2006a,b), except over the north-western regions in winter and spring and some continental areas in summer. The number of cyclone centers decreased in the A2 scenario except in summer, where it increased significantly because of increased levels of activity over land areas (mainly the Iberian and Balkan peninsulas). Fig. 17 shows the change of synoptic signal between the A2 and present climate simulations. The results confirm a change towards more stable conditions over most of the Mediterranean, except over the north-western areas during the cold season. These changes appear to be consistent with trends already detected during the second half of the 20th century (e.g. Trigo et al., 2006) and with what has been suggested by previous analyses of GCM output (Lionello et al. 2002; Pinto et al. in press).

#### 4.3. High resolution simulation

In this sub-section, we refer to the recent work of Gao et al. (2006), who reported on a high resolution (grid spacing of 20 km) climate change experiment over the Mediterranean region, which to date is the finest scale climate change scenario produced over the region.

One of the important messages of the work by Gao et al. (2006) is that the climate change signal over the Mediterranean shows substantial fine scale structure in response to the forcing of the complex topography of the region. This is illustrated by Fig. 18, which shows the simulated winter precipitation change and relates it to the change in low level circulation. Fig. 18 shows significant gradients in the magnitude and sign of the precipitation change signal across topographical systems, for example the Apennines in central Italy, the northeastern Alps and the Iberian plateau. These gradients are clearly associated with the low level circulation changes. The largest positive increases are found in the upwind sides of the topographical chains with respect to the direction of the prevailing circulation change, where precipitation is produced by uplift of humid air against the mountain slopes. Conversely, a minimum increase or even a decrease is

**Table 2**

Change in precipitation coefficient of variation ( $\Delta\sigma(P)$ ) and surface air temperature standard deviation ( $\Delta\sigma(T)$ ) averaged over the Mediterranean for the wet (October–March, O–M) and dry (April–September, A–S) seasons, different future time slices and different scenarios. The changes are calculated with respect to the 1961–1980 values and are expressed as percentage of the 1961–1980 value. Only land points are included in the calculations

		2001–2020	2021–2040	2041–2060	2061–2080	2081–2100
$Ds(P)$ O–M	B1	3.69	8.36	10.81	11.54	16.18
	A1B	7.61	9.64	13.68	17.31	21.57
	A2	3.86	14.98	9.80	26.80	37.08
$Ds(P)$ A–S	B1	10.40	15.29	32.87	22.96	28.01
	A1B	9.11	11.35	24.05	34.70	48.78
	A2	7.81	20.45	22.09	34.09	43.19
$Ds(T)$ O–M	B1	0.00	4.84	5.71	-2.33	-6.01
	A1B	3.46	1.90	-2.66	0.31	0.46
	A2	2.49	1.24	-7.61	-0.27	-4.73
$Ds(T)$ A–S	B1	-0.54	4.63	7.46	3.13	10.48
	A1B	4.66	3.88	5.80	13.05	20.72
	A2	-0.18	-5.39	6.73	9.82	14.56

## Surface air temperature (DT, C) and precipitation (DP, %) Change, 2071–2100 minus 1961–1990, A2 scenario

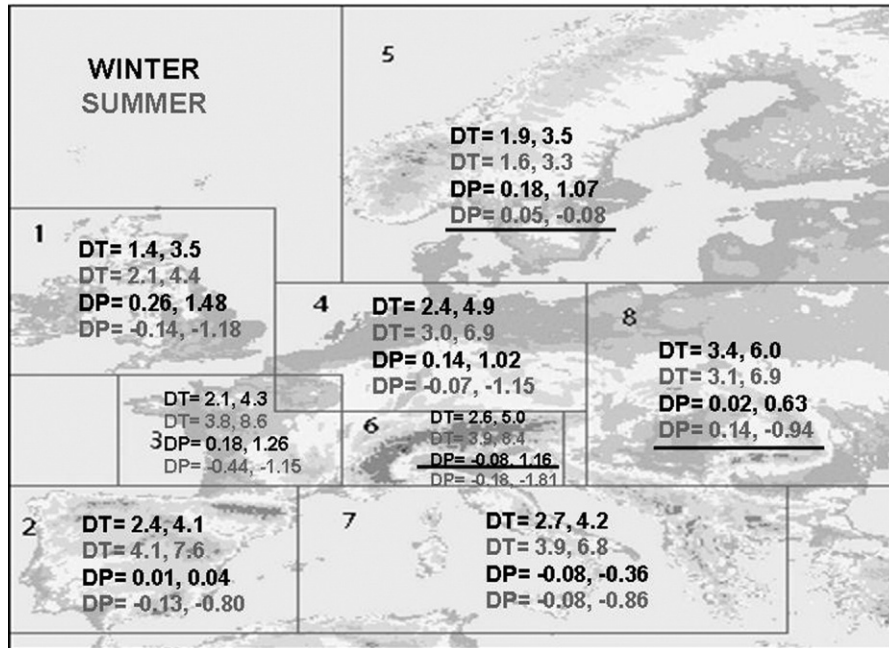


**Fig. 15.** Minimum and maximum change in surface air temperature (DT) and precipitation (DP) simulated by the ensemble of global and regional climate models in the PRUDENCE project over different PRUDENCE sub-regions (land only points), 2071–2100 minus 1961–1990, A2 scenario. Units are °C for temperature and mm/day for precipitation. Adapted from the data in Deque et al. (2005).

found on the corresponding lee side of the mountain chains. A similar fine scale forcing of the change signal was found also for the occurrence of drought and extreme precipitation events (Gao et al., 2006).

Comparison of the precipitation changes in Fig. 18 with those based on the MGME in Fig. 3 clearly shows that current AOGCMs are still too coarse to capture the fine scale structure of the climate change signal over the Mediterranean region. This has the important consequence that high resolution modeling is necessary to simulate surface climate change over the region for use in impact assessment studies. In this regard, it is worth mentioning that the quality of current RCM projections is often deemed sufficient to use RCM output in impact assessment studies (e.g. Mearns et al., 2001; Adams et al., 2003; Stone et al., 2003; Kleinn 2005).

### 5. Summary considerations and discussion

In this paper we have presented a review of climate change projections over the Mediterranean region based on the latest and most advanced sets of global and regional climate model simulations. These simulations give a collective picture of a substantial drying and warming of the Mediterranean region, especially in the warm season (precipitation decrease exceeding –25–30% and warming exceeding 4–5 °C). The only exception to this picture is an increase of precipitation during the winter over some areas of the northern Mediterranean basin, most noticeably the Alps. Inter-annual variability is projected to generally increase as is the occurrence of extreme heat and drought events. These signals are robust in that they are present in most projections from both global and regional models, and are consistent across emission scenarios and future time slices. In addition, this general signal has been found quite consistently also in previous generations of global (Kittel et al., 1998; Giorgi and Francisco 2000; Giorgi et al., 2001; Ulbrich et al., 2006) and regional (e.g. Giorgi et al., 1992; Jones et al., 1997; Deque et al., 1998; Machenhauer et al., 1998; Raisanen et al., 1999; Christensen and Christensen 2003; Semmler and Jacob 2004; Kjellstrom 2004; Schar et al., 2004; Giorgi

et al., 2004b; Raisanen et al., 2004; Deque et al., 2005) model projections. In this regard, we should recall that we have mostly analyzed the signal from ensembles of simulations. By definition, this filters out inter-decadal variability. As pointed out by Giorgi (2005), actual climate change will be only one “realization” possibly characterized by multi-decadal variability that should be superposed to the mean projected changes found here.

What are the physical processes underlying these projected changes? We have seen that the drying of the Mediterranean is associated with increasing anticyclonic circulation over the region which causes a northward shift of the mid-latitude storm track. This northward shift has a seasonal migration and it is maximum in summer and minimum in winter. The winter change pattern has characteristics consistent with those found during the positive phase of the NAO. Indeed, at least two previous studies (Terray et al., 2004;

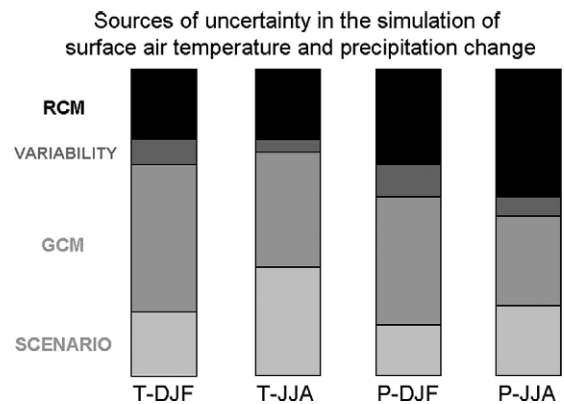


**Fig. 16.** Relative magnitude of the sources of uncertainty in the simulation of seasonal surface air temperature and precipitation change within the ensemble of PRUDENCE experiments for the whole European region. Adapted from the data in Deque et al. (2005).

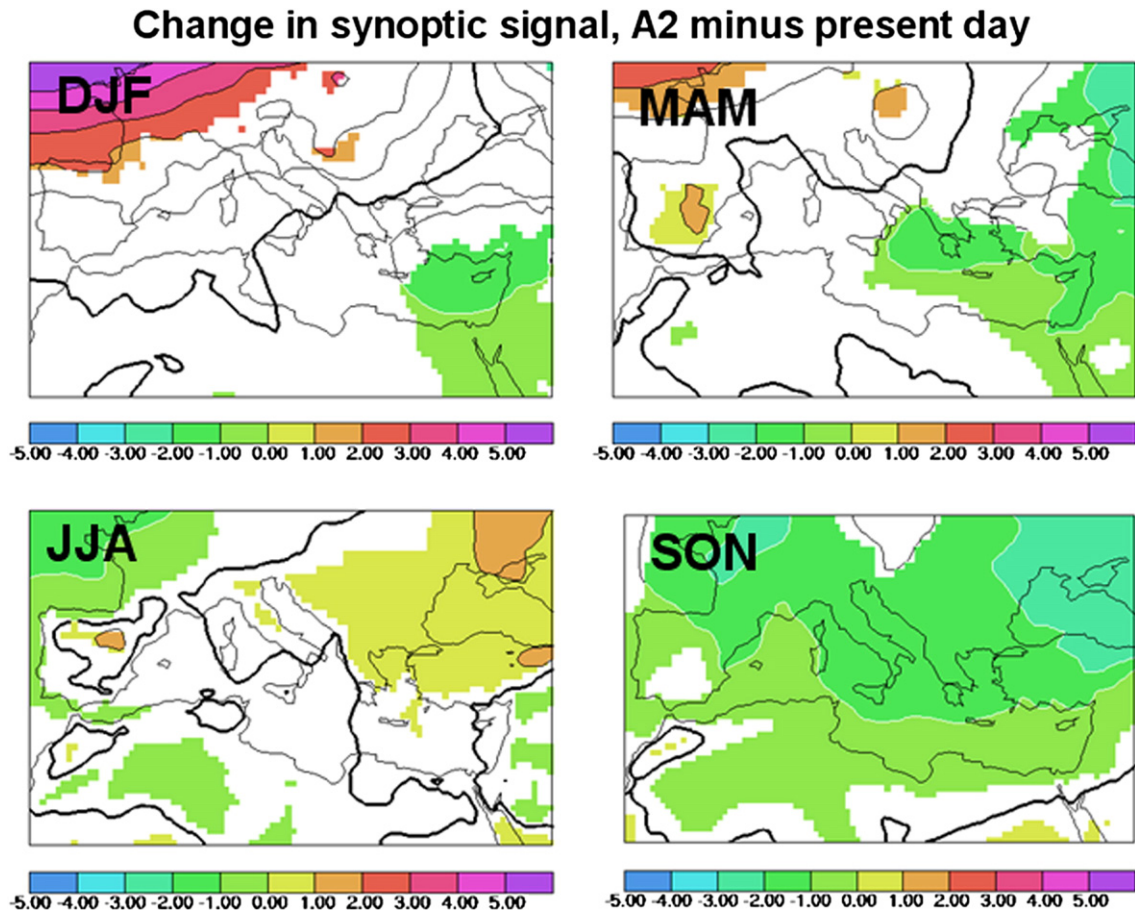


**Fig. 17.** Change in synoptic activity between A2 scenario and present day conditions in the simulations of Giorgi et al. (2004a,b). Colored areas indicate statistically significant differences at the 95% confidence level on the basis of a Mann–Whitney test. (For interpretation of the references to colour in this figure legend, the reader is referred to the web version of this article.)

Coppola et al., 2005) found an increase in the occurrence of positive NAO conditions in future climate simulations. In particular, Coppola et al. (2005) found the emergence of a bimodal distribution of NAO events in greenhouse gas forced scenario simulations, with the second mode located in the region of high positive NAO values. This would yield a tendency to increased occurrence of extreme seasons in the scenario projections, which would be consistent with the increased variability found in this study.

The causes for the large summer drying signal have been investigated by Rowell and Jones (2006), who examined four possible mechanisms: (1) Low spring soil moisture conditions leading to reduced summer convection; (2) large land-sea contrast in warming leading to reduced relative humidity and precipitation over the continent; (3) positive summer soil moisture precipitation feedback; and (4) remote influences (e.g. descending motions induced by the strengthening of the Asian monsoon). The first two were found to provide the dominant contributions, while remote effects were found to be only of minor importance. It is also possible that the greenhouse gas forcing is triggering a change in large scale wave patterns that enhance the occurrence of blocking like anticyclonic circulations over the northeastern Atlantic (Pal et al., 2004).

The change signals projected by current models for the Mediterranean region are large, consistent and increase with the magnitude of the forcing. As mentioned, the comparative analysis of Giorgi (2006) indeed places the Mediterranean among the most responsive regions to global climate change. Given that the Mediterranean is a transition area between the temperate climate of central Europe and the arid climate of northern Africa, such changes have the potential to profoundly modify the climate characteristics of the Mediterranean.

This, along with the potential of pronounced sea level rise under global warming, could have devastating effects on water resources, natural ecosystems (both terrestrial and marine), human activities (e.g. agriculture, recreation, tourism) and health. The evidence from model projections thus indicates that the Mediterranean might be an especially vulnerable region to global climate change and that this

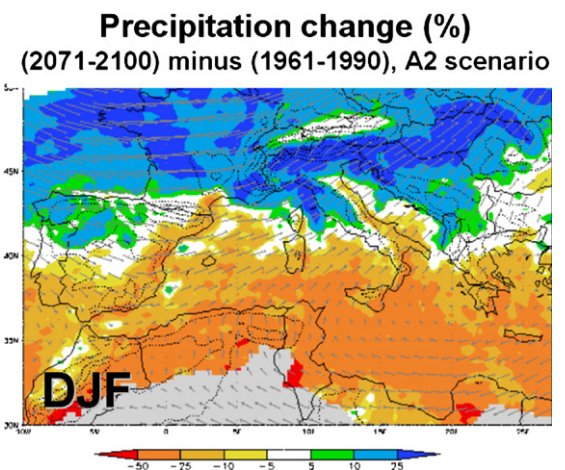


**Fig. 18.** Winter (DJF) precipitation change simulated over the Mediterranean region in the high resolution (20 km grid spacing) experiment of Gao et al. (2006). The changes are calculated between the periods of 2071–200 and 1961–1990 for the A2 scenario. Units are % of 1961–1990 value. The arrows indicate the corresponding change in 850 mb wind.

issue cannot be underestimated by the scientific and policy making community.

## Acknowledgements

We would like to thank X. Bi for technical support in producing some of the figures included in this paper and two anonymous reviewers for their constructive and useful comments.

## References

- Adams, R.M., McCarl, B.A., Mearns, L.O., 2003. The effects of spatial scales of climate scenarios on economic assessments: an example from U.S. agriculture. *Clim. Change* 60, 131–148.
- Alpert, P., et al., 2006. Relations between climate variability in the Mediterranean region and the Tropics: ENSO, South Asian and African monsoons, hurricanes and Saharan dust. In: Lionello, P., Malanotte-Rizzoli, P., Boscolo, R. (Eds.), *Mediterranean Climate Variability*. Elsevier, Amsterdam, pp. 149–177.
- Beniston, M., et al., 2007. Current and future extreme climatic events in Europe: observations and modeling studies conducted within the EU PRUDENCE project. *Clim. Change* 81, 71–95.
- Christensen, J.H., Christensen, O.B., 2003. Climate modeling: severe summertime flooding in Europe. *Nature* 421, 805–806.
- Christensen, J.H., Carter, T.R., Giorgi, F., 2002. PRUDENCE employs new methods to assess European climate change. *EOS* 83, 147.
- Coppola, E., Kucharski, F., Giorgi, F., Molteni, F., 2005. Bimodality of the North Atlantic Oscillation in simulations with greenhouse gas forcing. *Geophys. Res. Lett.* 32, L23709.
- Deque, M., Marquet, P., Jones, R.C., 1998. Simulation of climate change over Europe using a global variable resolution general circulation model. *Clim. Dyn.* 14, 173–189.
- Deque, M., et al., 2005. Global high resolution vs. regional climate model climate change scenarios over Europe: quantifying confidence level from PRUDENCE results. *Clim. Dyn.* 25, 653–670.
- Gao, X., Pal, J.S., Giorgi, F., 2006. Projected changes in mean and extreme precipitation over the Mediterranean region from high resolution double nested RCM simulations. *Geophys. Res. Lett.* 33, L03706.
- Giorgi, F., 2005. Interdecadal variability of regional climate change: implications for the development of regional climate change scenarios. *Meteorol. Atmos. Phys.* 89, 1–15.
- Giorgi, F., 2006. Climate change hot-spots. *Geophys. Res. Lett.* 33, L08707.
- Giorgi, F., Francisco, R., 2000. Evaluating uncertainties in the prediction of regional climate change. *Geophys. Res. Lett.* 27, 1295–1298.
- Giorgi, F., Bi, X., 2005a. Regional changes in surface climate interannual variability for the 21st century from ensembles of global model simulations. *Geophys. Res. Lett.* 32, L13701.
- Giorgi, F., Bi, X., 2005b. Updated regional precipitation and temperature changes for the 21st century from ensembles of recent AOGCM simulations. *Geophys. Res. Lett.* 32, L21715.
- Giorgi, F., Marinucci, M.R., Visconti, G., 1992. A 2XCO<sub>2</sub> climate change scenario over Europe generated using a limited area model nested in a general circulation model. II: climate change scenario. *J. Geophys. Res.* 97, 10011–10028.
- Giorgi, F., Marinucci, M.R., Bates, G.T., 1993a. Development of a second generation regional climate model (RegCM2). Part I: boundary layer and radiative transfer processes. *Mon. Weather Rev.* 121, 2794–2813.
- Giorgi, F., Marinucci, M.R., Bates, G.T., DeCanio, G., 1993b. Development of a second generation regional climate model (RegCM2). Part II: convective processes and assimilation of lateral boundary conditions. *Mon. Weather Rev.* 121, 2814–2832.
- Giorgi, F., Hurrell, J.W., Marinucci, M.R., Beniston, M., 1997. Elevation signal in surface climate change: a model study. *J. Clim.* 10, 288–296.
- Giorgi, F., et al., 2001. Emerging patterns of simulated regional climatic changes for the 21st century due to anthropogenic forcings. *Geophys. Res. Lett.* 28, 3317–3320.
- Giorgi, F., Bi, X., Pal, J.S., 2004a. Mean, interannual variability and trends in a regional climate change experiment over Europe. Part I: present day climate (1961–1990). *Clim. Dyn.* 22, 733–756.
- Giorgi, F., Bi, X., Pal, J.S., 2004b. Mean, interannual variability and trends in a regional climate change experiment over Europe. Part II: future climate scenarios (2071–2100). *Clim. Dyn.* 23, 839–858.
- Hurrell, J.W., 1995. Decadal trends in the North Atlantic Oscillation: regional temperature and precipitation. *Science* 269, 676–679.
- Intergovernmental Panel on Climate Change, 2000. In: Nakicenovic, N., et al. (Eds.), *Special Report on Emission Scenarios*. Cambridge University Pres, New York. 599 pp.
- Intergovernmental Panel on Climate Change, 2001. In: Houghton, J.T., Ding, Y., Griggs, D.J., Noguer, M., van der Linden, P.J., Dai, X., Maskell, K., Johnson, C.A. (Eds.), *Climate Change 2001: The Scientific Basis. Contribution of Working Group I to the Third Assessment Report of the Intergovernmental Panel on Climate Change*. Cambridge University Press, Cambridge. 881 pp.
- Jacobbeit, J., Dünkeloh, A., Hertig, E., 2005. Mediterranean rainfall changes and their causes. In: Losan, J., et al. (Ed.), *WarnsignalKlima: Genug Wasser für alle?* Hamburg, pp. 192–196.
- Jones, R.G., Murphy, J.M., Noguer, M., Keen, A.B., 1997. Simulation of climate change over Europe using a nested regional climate model. II: comparison of driving and regional model responses to a doubling of carbon dioxide. *Q. J. R. Meteorol. Soc.* 123, 265–292.
- Kittel, T.G.F., Giorgi, F., Meehl, G.A., 1998. Intercomparison of regional biases and doubled CO<sub>2</sub> sensitivities of coupled atmosphere–ocean general circulation model experiments. *Clim. Dyn.* 14, 1–15.
- Kjellstrom, E., 2004. Recent and future signatures of climate change in Europe. *Ambio* 33, 193–198.
- Kjellstrom, E., et al., 2007. Modeling daily temperature extremes: recent climate and future changes over Europe. *Clim. Change* 81, 249–265.
- Klein, J., 2005. Hydrologic simulations in the Rhine basin driven by a regional climate model. *J. Geophys. Res.* 110, D05108.
- Lionello, P., Dalan, F., Elvini, E., 2002. Cyclones in the Mediterranean region: the present and doubled CO<sub>2</sub> climate scenarios. *Clim. Res.* 22, 147–159.
- Lionello, P., et al., 2006a. The Mediterranean climate: an overview of the main characteristics and issues. In: Lionello, P., Malanotte-Rizzoli, P., Boscolo, R. (Eds.), *Mediterranean Climate Variability*. Elsevier, Amsterdam, pp. 1–26.
- Lionello, P., et al., 2006b. Cyclones in the Mediterranean region: climatology and effects on the environment. In: Lionello, P., Malanotte-Rizzoli, P., Boscolo, R. (Eds.), *Mediterranean Climate Variability*. Elsevier, Amsterdam, pp. 325–372.
- Luterbacher, J., et al., 2006. Mediterranean climate variability over the last centuries. A review. In: Lionello, P., Malanotte-Rizzoli, P., Boscolo, R. (Eds.), *Mediterranean Climate Variability*. Elsevier, Amsterdam, pp. 27–148.
- Machenauer, B., et al., 1998. Validation and Analysis of Regional Present-day Climate and Climate Change Simulations over Europe. . MPI Report No, 275. MPI, Hamburg, Germany.
- Mearns, L.O., Easterling, W., Hays, C., Marx, D., 2001. Comparison of agricultural impacts of climate change calculated from high and low resolution climate change scenarios. Part I: the uncertainty due to spatial scale. *Clim. Change* 51, 131–172.
- Mitchell, J.F.B., et al., 2001. Detection of climate change and attribution of causes. Chapter 12 of Intergovernmental Panel on Climate Change (IPCC), 2001: climate change 2001: the scientific basis. In: Houghton, J.T., Ding, Y., Griggs, D.J., Noguer, M., van der Linden, P.J., Dai, X., Maskell, K., Johnson, C.A. (Eds.), *Contribution of Working Group I to the Third Assessment Report of the Intergovernmental Panel on Climate Change*. Cambridge University Press, Cambridge, pp. 695–738.
- Mitchell, T.D., 2003. Pattern scaling. An examination of the accuracy of the technique for describing future climates. *Clim. Change* 60, 217–242.
- New, M.G., Hulme, M., Jones, P.D., 2000. Representing twentieth century space time climate fields. Part II: development of a 1901–1996 mean monthly terrestrial climatology. *J. Clim.* 13, 2217–2238.
- Pal, J.S., Small, E.E., Eltahir, E.A.B., 2000. Simulation of regional scale water and energy budgets: representation of sub-grid cloud and precipitation processes within RegCM. *J. Geophys. Res.* 29579–29594.
- Pal, J.S., Giorgi, F., Bi, X., 2004. Consistency of recent summer European precipitation trends at extremes with future regional climate projections. *Geophys. Res. Lett.* 31, L13202.
- Pinto, J.G., Spangherl, T., Ulbrich, U., Speth, P., in press. Assessment of winter cyclone activity in a transient ECHAM4-OPYC3 GHG experiment. *Meteorol. Zeitschrift*.
- Raisanen, J., 2002. CO<sub>2</sub> induced changes in interannual temperature and precipitation variability in 19 CMIP2 experiments. *J. Clim.* 15, 2395–2411.
- Raisanen, J., et al., 1999. The First Rossby Centre Regional Climate Scenario – Dynamical Downscaling of CO<sub>2</sub>-induced Climate Change in the HadCM2 GCM. . SHMI Reports Meteorology and Climatology No. 85. Swedish Meteorological and Hydrological Institute, Norrköping, Sweden. 56 pp, SE-601 76.
- Raisanen, J., et al., 2004. European climate in the late twenty-first century: regional simulations with two driving global models and two forcing scenarios. *Clim. Dyn.* 22, 13–31.
- Rotach, M.W., et al., 1997. Nested regional simulation of climate change over the Alps for the scenario of doubled greenhouse gas forcing. *Theor. Appl. Climatol.* 57, 209–227.
- Rowell, D.P., Jones, R.G., 2006. Causes and uncertainty of future summer drying over Europe. *Clim. Dyn.* 27, 281–299.
- Sanchez, E., Gallardo, C., Gaertner, M.A., Arribas, A., Castro, M., 2004. Future climate extreme events in the Mediterranean simulated by a regional climate model: a first approach. *Glob. Planet. Change* 44, 163–180.
- Schar, C., et al., 2004. The role of increasing temperature variability in European summer heatwaves. *Nature* 427, 332–336.
- Semmler, T., Jacob, D., 2004. Modeling extreme precipitation events – a climate change simulation for Europe. *Glob. Planet. Change* 44, 119–127.
- Stone, M.C., Hotchkiss, R.H., Mearns, L.O., 2003. Water yield response to high and low spatial resolution climate change scenarios in the Missouri River Basin. *Geophys. Res. Lett.* 30, 1186.
- Stott, P.A., 2003. Attribution of regional scale temperature changes to anthropogenic and natural causes. *Geophys. Res. Lett.* 30, 1728.
- Terray, L., Demory, M.E., Deque, M., de Coetlogon, G., Maisonneuve, E., 2004. Simulation of late 21st century changes in wintertime atmospheric circulation over Europe due to anthropogenic causes. *J. Clim.* 17, 4630–4645.
- Trigo, R., et al., 2006. Relations between variability in the Mediterranean region and mid-latitude variability. In: Lionello, P., Malanotte-Rizzoli, P., Boscolo, R. (Eds.), *Mediterranean Climate Variability*. Elsevier, Amsterdam, pp. 179–226.
- Xoplaki, E., 2002. Climate variability over the Mediterranean, PhD thesis, University of Bern, Switzerland, Available through: [http://sinus.unibe.ch/klimet/docs/phd\\_xoplaki.pdf](http://sinus.unibe.ch/klimet/docs/phd_xoplaki.pdf).
- Xoplaki, E., González-Rouco, J.F., Luterbacher, J., Wanner, H., 2004. Wet season Mediterranean precipitation variability: influence of large-scale dynamics and trends. *Clim. Dyn.* 23, 63–78.
- Ulbrich, U., et al., 2006. The Mediterranean climate change under global warming. In: Lionello, P., Malanotte-Rizzoli, P., Boscolo, R. (Eds.), *Mediterranean Climate Variability*. Elsevier, Amsterdam, pp. 398–415.